JOURNAL OF SOLID STATE CHEMISTRY 5, 276–285 (1972)

Phase Diagrams to 40 kbar and Crystallographic Data for $RbNO_2$ and $CsNO_2$*

P. W. RICHTER AND CARL W. F. T. PISTORIUS

Chemical Physics Group of the National Physical and National Chemical Research Laboratories, South African Council for Scientific and Industrial Research, P.O. Box 395, Pretoria, South Africa

Received November 4, 1971

$CsNO_2$ I at ambient conditions is cubic, space group O_h^1–$Pm3m$, with $a_0 = 4.389$ Å, and transforms at −94°C to rhombohedral $CsNO_2$ II, space group D_{3d}^5–$R\bar{3}m$, with $a_{rh} = 4.307$ Å, $\alpha = 87°22'$. The $CsNO_2$ II/I transition line rises with pressure. $RbNO_2$ I at ambient conditions is cubic, space group O_h^5–$Fm3m$, with $a_0 = 6.934$ Å. It transforms at −12°C to monoclinic $RbNO_2$ II with $a_0 = 8.904$, $b_0 = 4.828$, $c_0 = 8.185$ Å, $\beta = 115.7°$ at −62°C. $RbNO_2$ II appears to be ordered, whereas $RbNO_2$ I has a configurational entropy of $R\ln 32$. The $RbNO_2$ II/I transition line is terminated at 0.3 kbar with the appearance of $RbNO_2$ III which is 17.3% denser than $RbNO_2$ I. The $RbNO_2$ II/III transition pressure increases with decreasing temperature to a triple point at 1.2 kbar, −65°C where a further dense phase $RbNO_2$ IV appears. The $RbNO_2$ IV/III phase boundary is very similar to the $CsNO_2$ II/I boundary. The $RbNO_2$ II/IV transition pressure rises slightly with decreasing pressure. The melting curve of $RbNO_2$ I passes through a maximum at 2.2 kbar, 390°C, and is terminated at the $RbNO_2$ III/I/liquid triple point at 5.2 kbar, 382°C. The melting curve of $RbNO_2$ III rises steeply with pressure.

1. Introduction

The complex polymorphism of the alkali nitrites affords considerable insight into the variety of order–disorder phenomena related to orientation of V-shaped anions in ionic crystals. By far the most thoroughly studied example is $NaNO_2$, due mainly to the discovery of ferroelectricity in this compound at ambient conditions (*1*). Ferroelectric $NaNO_2$ III is orthorhombic, space group C_{2v}^{20}–$Im2m$ (*2–4*). The spontaneous polarization is parallel to the b_0 axis, while the NO_2^- ions lie parallel to one another in the planes perpendicular to the a_0 axis. At the ferroelectric Curie point (163.4°C) the substance transforms to antiferroelectric $NaNO_2$ II in which the ordering parameter of the ions in the a_0 plane changes sinusoidally along the a_0 axis with a period of ~8 layers. At the Néel temperature (164.7°C) a further transformation occurs to paraelectric $NaNO_2$ I, which is also orthorhombic, but with the higher symmetry space group D_{2h}^{25}–$Immm$ (*7*), due to oscillation of the ions along the b_0 axis. The sodium and nitrogen atoms can be considered to occupy half the 4*g* positions, while the oxygen atoms are distributed over half the 8*l* positions. Gesi et al. (*8*) found that both the Curie and Néel temperatures rise with pressure to 10 kbar, and that the narrow stability region of $NaNO_2$ II increases with pressure. This was confirmed by Rapoport (*9*) to 40 kbar. Rapoport also discovered a new phase $NaNO_2$ V just below the melting curve at pressures above 9.4 kbar (*10*). Finally, $NaNO_2$ IV is found upon compressing $NaNO_2$ III (*9*, *11*). The III/IV transition appears to be of the second order. The transition line meets the temperature axis at −96°C (*12*).

KNO_2 I above 39°C (*13*) is cubic, space group O_h^5–$Fm3m$ (*14*). KNO_2 II is rhombohedral (*15*), space group D_{3d}^5–$R\bar{3}m$ (*14*). Both these phases are disordered, KNO_2 II with a configurational entropy of $R\ln 6$ (*14*) or $R\ln 12$ (*16*) and KNO_2 I with $R\ln 32$ (*14*). Two monoclinic (*14*, *16*) phases KNO_2 III and VII are stable below −13°C (*17*),

* Based on part of a dissertation to be submitted by one of us (PWR) in partial fulfilment of the requirements for the Ph.D. degree at the University of South Africa.

and at −100°C (*16*), respectively. At elevated pressures (*9*) all these phases transform to considerably denser phases which are related to the CsCl-type structure (*18*). KNO_2 V occurs above ~75°C, and KNO_2 IV below this temperature. The IV/V transition line splits at 27.3 kbar, 75°C (*9*, *10*), with the appearance of KNO_2 VI. KNO_2 V is cubic, space group O_h^1–*Pm3m*, while KNO_2 IV and VI are only partly disordered (*18*). A final point of interest here is that the melting curve of KNO_2 I has a pronounced maximum (*9*). The falling part of the melting line is terminated at the V/I/liquid triple point at 14.9 kbar.

We are not aware of any work relating to the crystallography or polymorphism of $RbNO_2$. $CsNO_2$ at ambient conditions is cubic, space group O_h^1–*Pm3m* (*19*). This is the same arrangement as that of KNO_2 V (*18*). Using the arguments set out elsewhere (*20*), one can expect to find a low-temperature phase of $CsNO_2$ with the same structure as KNO_2 IV. $RbNO_2$ should behave in a fashion intermediate between $CsNO_2$ and KNO_2.

2. Experimental

$RbNO_2$ and $CsNO_2$ with stated purities of 99% were obtained from Rocky Mountain Research, Inc., further purified by fractional recrystallization from aqueous solution, and thoroughly dried.

X-Ray powder diffraction patterns at 25°C were obtained in a Philips high angle diffractometer. Patterns at lower temperatures were obtained by mounting samples, sealed in Lindemann tubes, in a Weissenberg camera and cooling by means of a current of cold nitrogen. Temperatures were measured with a thermocouple junction ~0.5 mm from the sample. The low-temperature diffraction photographs obtained in this way were corrected for absorption and film shrinkage by photographing the 25°C pattern of the same sample onto the same film in each case, and comparing the spacings with those obtained in the diffractometer.

Pressures up to 40 kbar were generated in a piston–cylinder apparatus (*21*). Phase changes with relatively large volume changes were studied by volumetric methods (*22*), while those with smaller volume changes were studied by differential thermal analysis (DTA), using Chromel–Alumel thermocouples. The samples were packed into nickel and stainless steel capsules in a dry box. Heating/cooling rates ranged from 0.3–1.5 deg/sec. The detailed experimental arrangement has been described before (*23*). Solid–solid phase boundaries were taken to be the mean of heating and cooling temperatures and were based on several consistent runs. The final boundaries are believed to be better than ±2 deg and ±0.5 kbar.

3. Crystallography

The observed peaks of $CsNO_2$ I at 25°C could be explained on the basis of a bcc unit cell, space group O_h^1–*Pm3m*, in agreement with Ferrari et al. (*19*). Our lattice constant is higher, though, being 4.389 ± 0.003 Å as compared to 4.34 Å found by the previous workers. The calculated density, taking $Z = 1$, is 3.514 g/cm^3. The powder pattern of $CsNO_2$ I is given in Table I.

The powder pattern of $CsNO_2$ at −151°C was different from that at 25°C, indicating a phase transition to a new phase $CsNO_2$ II between these temperatures. The powder pattern at −151°C could be explained on the basis of a rhombohedral unit cell with $a_{rh} = 4.307 \pm 0.015$ Å, $\alpha_{rh} = 87° 22' \pm 20'$, and is given in Table II. The calculated density, taking $Z = 1$ here also, is 3.729 g/cm^3.

The configurational entropy required by an assumption of one-dimensional "free" rotation

TABLE I

POWDER PATTERN OF $CsNO_2$ I AT 25°C (FILTERED CuK_α RADIATION)

d_{obs} (Å)	d_{calc} (Å)	$h\,k\,l$	I
4.41	4.389	1 0 0	33
3.104	3.103	1 1 0	100
2.535	2.5339	1 1 1	88
2.1945	2.1944	2 0 0	32
1.9628	1.9627	2 1 0	21
1.7911	1.7917	2 1 1	23
1.5520	1.5517	2 2 0	7
1.4627	1.4629	2 2 1	11
1.3881	1.3879	3 1 0	4
1.3232	1.3233	3 1 1	3
1.2669	1.2669	2 2 2	1
1.2169	1.2172	3 2 0	2
1.1731	1.1730	3 2 1	3
1.0974	1.0973	4 0 0	<1
1.0649	1.0646	4 1 0	1
1.0342	1.0345	4 1 1, 3 3 0	1
0.9814	0.9814	4 2 0	<1

TABLE II

POWDER PATTERN OF $CsNO_2$ II AT −151°C (FILTERED CuK_α RADIATION)

d_{obs} (Å)	d_{calc} (Å)	$h\,k\,l$[a]	I
4.30	4.298	0 0 1	VS
3.10	3.108	0 1 1	VVS
2.96	2.974	0 1 $\bar{1}$	VVS
2.61	2.598	1 1 1	VW
2.450	2.449	1 1 $\bar{1}$	W
2.151	2.149	0 0 2	S
1.957	1.957	0 1 2	M
1.884	1.889	0 1 $\bar{2}$	M
1.827	1.823	1 1 2	W
1.742	1.742	1 2 $\bar{1}$	S
1.555	1.554	0 2 2	W
1.493	1.492	1 2 2	S
1.432	1.433	0 0 3, 1 $\bar{2}$ $\bar{2}$	W
1.405	1.406	1 2 $\bar{2}$	W
1.378	1.378	0 1 3	VW
1.337	1.342, 1.334	0 1 $\bar{3}$, 1 1 3	S
1.289	1.291	1 $\bar{1}$ 3	VW
1.218	1.217	0 2 3	W
1.189	1.190	1 2 3	W

[a] Rhombohedral indexing.

of the NO_2 groups in $CsNO_2$ II at −151°C is too high to be reasonable. The simplest and most obvious model for the structure of $CsNO_2$ II is to put the Cs^+ ion at the 1*a* (0,0,0) position of D_{3d}^5–$R\bar{3}m$, the N atom at the 1*b* ($\frac{1}{2},\frac{1}{2},\frac{1}{2}$) position, and to distribute the two O atoms among the two triplets of 6*h* (*xxz*; *xzx*; *zxx*; $\bar{x}\bar{x}\bar{z}$; $\bar{x}\bar{z}\bar{x}$; $\bar{z}\bar{x}\bar{x}$) positions. This model involves three distinct positions of the nitrite group, and therefore has a configurational entropy of $R\ln 3$, a value which appears to be quite acceptable. A higher configurational entropy could be yielded by a somewhat similar model which contains the N atom statistically distributed among the 6*h* positions with $x \sim z \sim \frac{1}{2}$. The proposed structure is, in either case, obviously closely related to the CsCl-type arrangement. Taking the effective ionic radius of eight-coordinated Cs^+ as 1.82 Å (*24*), the NO_2^- ellipsoid of rotation has a length of 4.16 Å and a diameter of 3.23 Å.

The observed peaks of $RbNO_2$ I at 25°C could be explained on the basis of a fcc unit cell, space group O_h^5–$Fm3m$, with $a_0 = 6.934 \pm 0.005$ Å. This phase can be expected to have the same structure as KNO_2 I, for which Solbakk and Strømme (*14*) suggested a configurational entropy

TABLE III

POWDER PATTERN OF $RbNO_2$ I AT 25°C (FILTERED CuK_α RADIATION)

d_{obs} (Å)	d_{calc} (Å)	$h\,k\,l$	I
4.00	4.004	1 1 1	19
3.467	3.465	2 0 0	100
2.4521	2.4517	2 2 0	37
2.0897	2.0908	3 1 1	12
2.0014	2.0018	2 2 2	5
1.7336	1.7336	4 0 0	3
1.5914	1.5909	3 3 1	3
1.5510	1.5506	4 2 0	3
1.4158	1.4155	4 2 2	1
1.3339	1.3345	5 1 1	1
1.2259	1.2259	4 4 0	<1
1.1722	1.1721	5 3 1	<1

of $R\ln 32$ on the basis of the only logically acceptable proposed atomic arrangement. The calculated density of $RbNO_2$ I, taking $Z = 4$, is 2.619 g/cm³. The powder pattern of $RbNO_2$ I at 25°C is given in Table III.

Powder diffraction patterns of $RbNO_2$ obtained at −20, −62, −103 and −130°C were all similar, but very different from that of $RbNO_2$ I at 25°C. This indicates a phase transition to a new phase $RbNO_2$ II between 25 and −20°C. The low-temperature patterns could not be explained on the basis of any cell with fewer than four independent variables. In particular, this phase is not similar to rhombohedral KNO_2 II or to orthorhombic $NaNO_2$ I or III. However, a monoclinic indexing was suggested by the fact that the low-temperature form of RbCN and the metastable low-temperature form of KCN are monoclinic (*25*). In fact, the present patterns could be indexed with ease on this basis when allowance was made for a change in space group due to the V-shaped NO_2^- ions as compared with rodlike CN^- ions. The monoclinic phase of KCN has the cell dimensions

$$a_0 = 8.04 \text{ Å}, \quad b_0 = 4.53 \text{ Å}, \quad c_0 = 7.47 \text{ Å}, \quad \beta = 109° 26',$$

whereas the present patterns of $RbNO_2$ II could be fitted by

$$a_0 = 8.904 \pm 0.012 \text{ Å}$$
$$b_0 = 4.828 \pm 0.010 \text{ Å}$$
$$c_0 = 8.185 \pm 0.012 \text{ Å}$$
$$\beta = 115.7 \pm 0.5°$$

at −62°C, and

$$a_0 = 8.905 \pm 0.015 \text{ Å}$$
$$b_0 = 4.847 \pm 0.012 \text{ Å}$$
$$c_0 = 8.185 \pm 0.012 \text{ Å}$$
$$\beta = 115.7 \pm 0.6°$$

at −103°C. The powder patterns at these temperatures are given in Table IV. It is clear that the lattice is primitive, but the space group cannot uniquely be determined in the absence of observed $0k0$ reflections. There appear to be no restrictions on hkl and $h0l$ reflections. Taking $Z = 4$, the density of $RbNO_2$ II is 2.75 g/cm³ at −62°C and 2.76 g/cm³ at −103°C. It must be emphasized here that any monoclinic assignment of a complex powder pattern must be regarded as tentative until confirmed by single-crystal studies.

TABLE IV

POWDER PATTERNS OF $RbNO_2$ II AT −62°C AND −103°C (FILTERED CuK_α RADIATION)

At −62°C			At −103°C			
d_{obs} (Å)	d_{calc} (Å)	I	d_{obs} (Å)	d_{calc} (Å)	I	$h\,k\,l$
4.39	4.419	M	4.39	4.417	S	$2\,0\,\bar{1}$
3.99	4.011, 4.010	S	3.98	4.016, 4.011	S	$1\,1\,\bar{1}$, $2\,0\,0$
3.58	3.603	W				$2\,0\,\bar{2}$
			3.32	3.305	W	$1\,1\,1$
3.13	3.121	VS	3.11	3.115	S	$1\,1\,\bar{2}$
2.97	2.959	M	2.95	2.959	M	$3\,0\,\bar{1}$
2.826	2.824	VS	2.81	2.819	VS	$3\,0\,\bar{2}$
2.694	2.701	M	2.678	2.680	M	$1\,0\,\bar{3}$
2.464	2.458	M	2.441	2.439	S	$0\,0\,3$
2.310	2.312	W				$1\,2\,0$
			2.299	2.301, 2.296	W	$0\,2\,1$, $1\,2\,\bar{1}$
2.225	2.223	VW				$3\,0\,1$
			2.204	2.208	VW	$4\,0\,\bar{2}$
2.149	2.151	VVW	2.149	2.145	VVW	$3\,1\,\bar{3}$
			2.069	2.074	VVW	$2\,2\,0$
2.003	2.005	M	1.998	1.997	M	$4\,0\,0$
			1.893	1.888	VW	$2\,2\,1$
1.856	1.857	VW				$1\,2\,2$
1.853	1.852	VW	1.852	1.853	VW	$4\,1\,0$
1.751	1.752	W	1.748	1.750	W	$4\,0\,1$
1.690	1.688	W	1.682	1.682	VW	$4\,1\,\bar{4}$
			1.611	1.612	VW	$3\,0\,\bar{5}$
1.602	1.604, 1.603	VVW				$5\,0\,0$, $5\,0\,\bar{4}$
1.540	1.542	VVW	1.542	1.545	VW	$4\,2\,0$
1.346	1.347	VVW	1.341	1.342	VW	$3\,2\,\bar{5}$
1.320	1.320	VVW				$1\,2\,\bar{5}$
1.240	1.238, 1.239, 1.239	VVW				$5\,2\,5$, $5\,2\,1$, $5\,1\,2$

4. Phase Boundaries

$CsNO_2$

The $CsNO_2$ I/II transition was observed at −94 ± 2°C at atmospheric pressure, this value being the mean of six determinations by means of DTA. The transition gave rise to strong signals both on heating and on cooling [Fig. 1(i)]. The temperatures obtained on heating were usually slightly lower than those obtained on cooling. This may indicate that the material used contained some nitrate as an impurity. The transition line is shown in Fig. 2. It rises with pressure with an initial slope of 4.9 deg/kbar and a small normal curvature. The observed points are summarized in the form of a power series in Table V.

No reliable points could be obtained on the melting curve of $CsNO_2$ I. This may have been due to the effect of nitrate impurity, or it may have been due to partial decomposition of the samples at elevated temperatures. The second

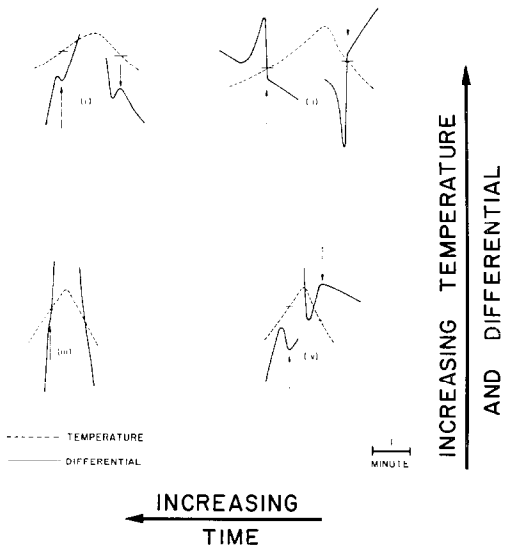

FIG. 1. Typical DTA signals obtained. (i) $CsNO_2$ II/I transition at 0 kbar, −97°C heating, −90.5°C cooling; (ii) $RbNO_2$ II/I transition at 0 kbar, −8.4°C heating, −24.8°C cooling; (iii) $RbNO_2$ I/liq at 3.5 kbar, 388°C; (iv) $RbNO_2$ IV/III transition at 28.2 kbar, 84°C heating, 95°C cooling.

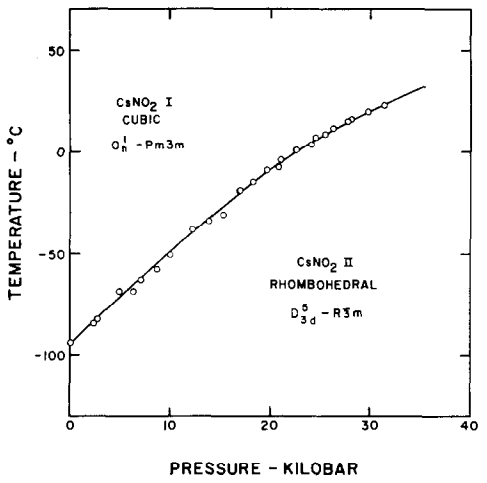

FIG. 2. $CsNO_2$ II/I transition line to 40 kbar.

alternative is the more likely in view of the fact that the first melting signal obtained for each sample was considerably sharper than later ones.

$RbNO_2$

The phase diagram of $RbNO_2$ is shown in Fig. 3. The $RbNO_2$ II/I transition was observed at -12 ± 2°C at atmospheric pressure, and exhibited a thermal hysteresis of 8–16 degrees. It yielded very strong DTA signals [Fig. 1(ii)] which were abruptly terminated at 0.3 kbar, −12°C.

Doubtful indications of further transitions at atmospheric pressure were given by weak DTA signals at −36 and −78°C. However, since the X-ray powder diffraction patterns at −20, −62, −103 and −130°C were similar, apart from thermal expansion, no major change occurs in this region.

The termination of the $RbNO_2$ II/I transition line at 0.3 kbar, with no DTA signals observed at immediately higher pressures, is obviously due to the intersection at this point of the II/I transition line with a new transition line carrying a large volume change. A search was made for this line by means of volumetric techniques. A typical compression curve at 126.4°C is shown in Fig. 4. The new $RbNO_2$ I/III transition has the very large volume change of 8.7 cm^3/mole, i.e. 17.3% of the molar volume of $RbNO_2$ I at 25°C. The transition, after piston rotation, occurs at 2.465 ± 0.040 kbar at 126.4°C, 1.917 ± 0.109 kbar at 81°C, and was encountered at 0.751 ± 0.025 kbar at 15.6°C on increasing pressure only. The reverse transition at this temperature was at too low a pressure to initiate, due to frictional effects. The $RbNO_2$ I/III phase boundary has a mean slope of 80 deg/kbar if linearity is assumed.

The $RbNO_2$ II/III transition line below −12°C was reversed once only due to the low transition pressure and frictional effects at low temperatures. The piston-rotation value obtained at −38°C was 0.65 ± 0.46 kbar. At still lower

TABLE V

PHASE RELATIONS OF $CsNO_2$ AND $RbNO_2$

Transition line	Fit	Standard deviation (°C)
$CsNO_2$ II/I	t (°C) $= -94 + 4.9P - 0.036P^2$	1.9
$RbNO_2$ II/I	t (°C) $= -12$	—
$RbNO_2$ IV/III	t (°C) $= -65 + 7.0(P - 1.2) - 0.046(P - 1.2)^2$	0.6
$RbNO_2$ II/IV	P (kbar) $= 1.2 - 0.0062(t + 65)$	—
$RbNO_2$ II/III	P (kbar) $= 0.3 - 0.0170(t + 12)$	—
$RbNO_2$ I/III	P (kbar) $= 0.3 + 0.0124(t + 12)$	—
$RbNO_2$ I/liq	t (°C) $= 385 + 4.4P - 1.00P^2$	2.0
$RbNO_2$ III/liq	t (°C) $= 382 + 27(P - 5.2) - 1.09(P - 5.2)^2$	0.6

Triple point	Pressure (kbar)[a]	Temperature (°C)[a]
$RbNO_2$ III/II/I	0.3	−12
$RbNO_2$ IV/II/III	1.2	−65
$RbNO_2$ III/I/liq	5.2	382

[a] The uncertainties corresponding to these values are best judged from Fig. 3.

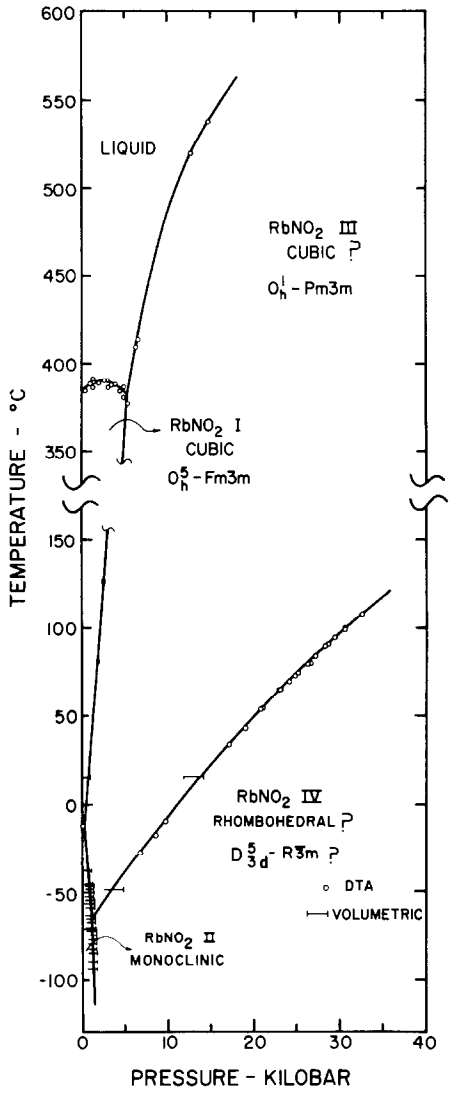

FIG. 3. Phase diagram of $RbNO_2$ to 40 kbar.

temperatures the transition could only be observed on compression. These piston-rotation points are shown in Fig. 3. The II/III transition pressure increases with decreasing temperature.

A slight change in the slope of the II/III transition line at 1.2 kbar, −65°C marks the $RbNO_2$ IV/II/III triple point. The $RbNO_2$ II/IV transition line is somewhat steeper than the II/III transition line. The new $RbNO_2$ IV/III transition was observed both by means of volumetric methods and by means of DTA. A typical compression–decompression cycle at 15.6°C is shown in Fig. 5. Due to the small volume change of the transition no attempt was made to relieve friction by means of piston rotation. The transition pressure at this temperature was 13.0 ± 1.1 kbar. The volume change of the IV/III transition was 0.61 cm^3/mole.

Typical DTA signals due to the IV/III transition are shown in Fig. 1(iv). The heating points were randomly 4–15° *lower* than the cooling points. The most obvious explanation of this effect is an impurity soluble in $RbNO_2$ III but not in $RbNO_2$ IV. However, the DTA peaks were sharp and relatively narrow, contrary to what would be expected for a two-phase region. The points plotted represent the means of heating and cooling transition temperatures, and are in good agreement with the volumetric points (Fig. 3). The $RbNO_2$ IV/III transition line rises with pressure, with gentle normal curvature. It was followed to 32.5 kbar, 108°C.

Melting and freezing of $RbNO_2$ yielded very weak DTA signals [Fig. 1(iii)]. Freezing signals were usually more pronounced, and were used to plot the melting curve. However, melting temperatures were in good agreement with freezing temperatures where it was possible to measure both. The melting curve of $RbNO_2$ I rises with pressure from an estimated value of 385°C at atmospheric pressure, passes through a maximum at ~2.2 kbar, 390°C and then falls with pressure to the $RbNO_2$ III/I/liquid triple point at 5.2 kbar, 382°C. The melting curve of $RbNO_2$ III rises steeply with pressure. The phase relations of $RbNO_2$ are summarized in Table V.

Discussion

The very large volume change of the $RbNO_2$ I/III transition can only be due to a coordination change at the transition. We suggest that $RbNO_2$ III is cubic with a CsCl-like disordered structure, space group O_h^1–*Pm3m*, as are the corresponding phases KNO_2 V (*18*) and $CsNO_2$ I. From the volumetric relations the lattice constant of $RbNO_2$ III at 25°C, ~1 kbar will be ~4.08 Å.

The mean slope of the $RbNO_2$ I/III transition line is 80 deg/kbar. Using the observed volume change of 8.7 cm^3/mole, the Clapeyron–Clausius relation yields

$$\Delta S_{III/I} = 10.8 \text{ J/deg mole}$$

for the entropy of transition, as compared to 6.3 J/deg mole for the corresponding KNO_2 I/V transition (*18*). It can be expected that the configurational entropies of $RbNO_2$ I and KNO_2 I are similar, with a configurational term of $R\ln 32$

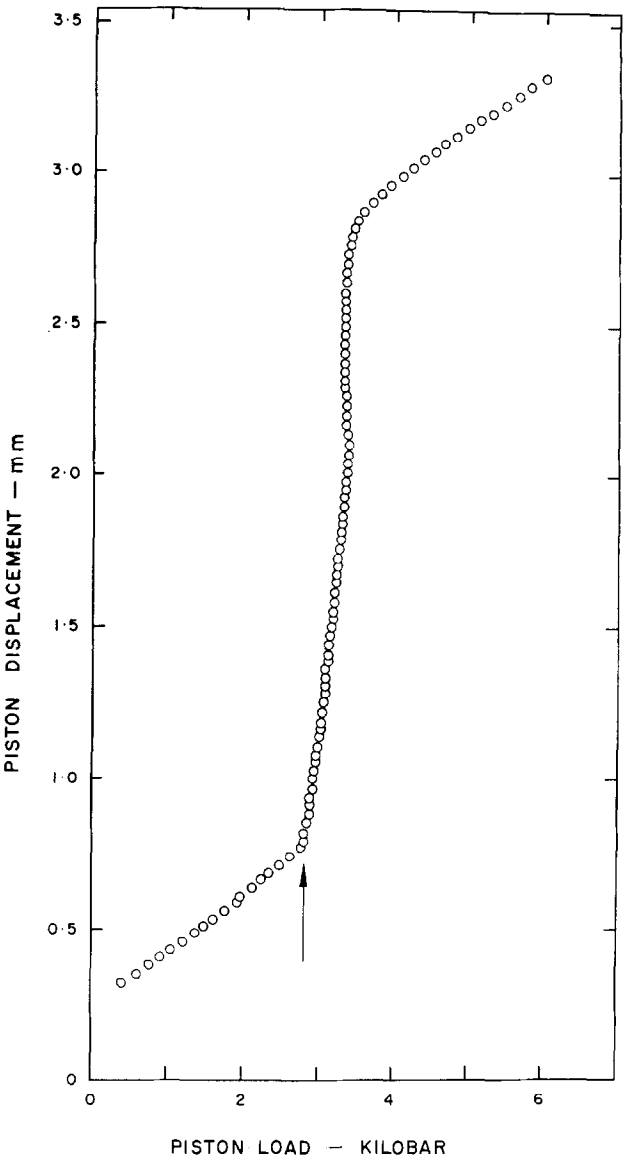

FIG. 4. Typical curve of piston displacement vs. load obtained upon compressing $RbNO_2$ at 126.4°C, showing the new I/III transition.

(*14*) if all possible configurations are sterically independent, or somewhat less if this is not the case. KNO_2 V was suggested (*18*) to have a configurational entropy of $R\ln 12$ if, with the cation in the 1*a* (0,0,0) position of *Pm*3*m* and the N atom in the 1*b* ($\frac{1}{2},\frac{1}{2},\frac{1}{2}$) position, the oxygens are in the 24 *m* positions. KNO_2 IV has the same space group (*18*) as $CsNO_2$ II and, probably, $RbNO_2$ IV. The configurational entropy for this arrangement is almost certainly $R\ln 3$. The experimental value of $\Delta S_{IV/V}$ for KNO_2 is slightly less than $R\ln 6$. However, the slope of the $RbNO_2$ IV/III transition line at 13.6 kbar, viz., 5.8 deg/kbar, together with the volume change of 0.61 cm^3/mole at this point, yields a transition entropy of 10.3 J/deg mole, quite close to $R\ln 4$. This strongly favours the arrangement for $RbNO_2$ III with a configurational entropy of $R\ln 12$. The initial volume change of the $RbNO_2$ IV/III transition at the III/IV/II triple point, assuming the entropy change to be roughly constant along the transition line, is

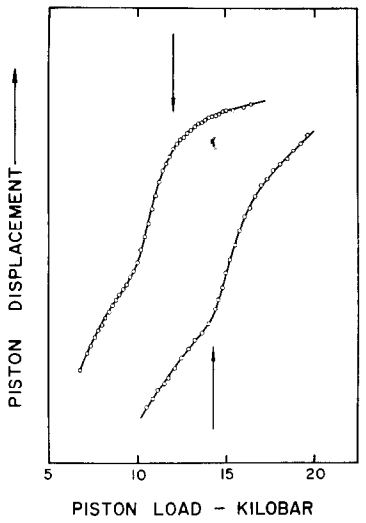

FIG. 5. Typical compression–decompression cycle for $RbNO_2$ at 15.6°C, showing the new III/IV transition.

0.73 cm^3/mole from the ratio of the slopes at 1.2 and 13.6 kbar. The initial slope of the $CsNO_2$ II/I transition line is 4.9 deg/kbar. If the entropy of the $CsNO_2$ II/I transition also is taken as $R\ln 4$, the volume change at the transition is found to be ~0.6 cm^3/mole. This value is not inconsistent with the X-ray results if allowance is made for thermal expansion.

The usual assumption made for the entropy of order–disorder transformations is that $\Delta S_{vibr} = 0$ in the expression (*26*)

$$\Delta S_{tr} = R\ln(N_2/N_1) + \Delta S_{vibr}$$

This approximation can be expected to be excellent in the case of the $CsNO_2$ II/I, $RbNO_2$ IV/III and $RbNO_2$ II/I transitions, since only slight structural changes are involved. However, in the case of transitions from 6- to 8-coordinated structure types, such as the $RbNO_2$ I/III, II/IV, or II/III transitions, this approximation is less valid. If all detail concerning the NO_2^- ion is neglected, $RbNO_2$ I and III can be considered as analogous to the B1 and B2 phases, respectively, of the alkali halides. Bassett et al. (*27*) showed that in that case, for which $R\ln(N_2/N_1) = 0$,

$$(\Delta S)_p \simeq \gamma_{01} C_{V1}(\Delta V/V_{01}) + (\Delta S)_V$$

where $(\Delta S)_p$ is the entropy difference at constant pressure, $(\Delta S)_V$ the entropy difference at constant volume due to structural reasons only, γ_{01} the Grüneisen parameter of the B1 phase, C_{V1} its specific heat at constant volume, and $\Delta V/V_{01}$ the relative volume change of the B1/B2 transition. Within their approximation, $(\Delta S)_V = 9.42$ J/deg mole. If we assume $\gamma_{01} \simeq 1.5$ similar to the value for the alkali halides (*28*), and $C_{V1} = 50$ J/deg mole (the Dulong–Petit value), the present value of $\Delta V/V_{01} = -0.173$ yields $S_{III} - S_I = -3.6$ J/deg mole. This means that the configurational part of $\Delta S_{III/I}$ equals 7.2 J/deg mole, or very closely $R\ln(32/12)$, as expected from the arguments above.

The volume change of the $RbNO_2$ II/I transition was too small to observe as a nonzero slope of the short transition line. If we therefore assume that $\Delta V_{II/I} \simeq 0$, it follows that $\Delta V_{II/III} \simeq \Delta V_{I/III} = -8.7$ cm^3/mole. The slope of the $RbNO_2$ II/III transition line is ~–60 deg/kbar, yielding

$$\Delta S_{II/III} \simeq 14.5 \text{ J/deg mole.}$$

From the relations at the $RbNO_2$ III/II/I triple point, therefore,

$$\Delta S_{II/I} \simeq 25.3 \text{ J/deg mole,}$$

which is intermediate between $R\ln 16$ (23 J/deg mole) and $R\ln 32$ (28.8 J/deg mole). We have no local facilities to determine $\Delta S_{II/I}$ directly and accurately in order to obtain a better value. The present inferred value of $\Delta S_{II/I}$ is consistent both with an ordered arrangement for $RbNO_2$ II and with an arrangement with a configurational entropy of $R\ln 2$. However, the present slope of the $RbNO_2$ II/IV transition is ~–160 deg/kbar, and from the additive relations at the $RbNO_2$ III/IV/II triple point $\Delta V_{II/IV} = -9.4$ cm^3/mole, yielding

$$\Delta S_{II/IV} = 5.8 \text{ J/deg mole.}$$

Eliminating the structural contribution of ~–3.6 J/deg mole, this yields ~9.4 J/deg mole for the configurational part of the entropy change, closely equal to $R\ln 3$ (9.1 J/deg mole). Since $RbNO_2$ IV must have a configurational entropy of $R\ln 3$ if it is isostructural with KNO_2 IV and $CsNO_2$ II, as would seem probable, this indicates that $RbNO_2$ II is ordered.

The maximum in the melting curve of $RbNO_2$ I is not unexpected in view of the maximum previously found in the melting curve of the corresponding phase KNO_2 I (*9*). In terms of Rapoport's model (*29*) for melting curve maxima at high pressures, these can be explained by assuming that, on a short-range basis, the liquid even at low pressures contains aggregates of CsCl-like as well as NaCl-like arrangements. Rapoport (*29*) showed that the concentration of

the denser CsCl-like aggregates can be expected to increase rapidly, albeit continuously, with pressure along the melting curve at the expense of the less dense NaCl-like aggregates, thus resulting, at and beyond the maximum, in a liquid which is more dense than the solid. As appears always to be the case, this behaviour is accompanied by a solid–solid transition with a large volume change.

There are indications that our materials may have contained some nitrate impurity. If so, the melting points will be low, but the essential features of the phase diagrams can be expected to be correct.

The present results largely confirm the basic ideas with regard to the interplay between coordinational polymorphism and ordering previously suggested (*20*). In KNO_2 (*9*, *18*, *30*) there are a group of NaCl-like phases at low pressures, with increasing disorder towards higher temperatures. Above ~10 kbar only denser CsCl-like phases are encountered. $RbNO_2$ shows essentially the same behaviour, but without a phase similar to the partly disordered rhombohedral KNO_2 II in the low-pressure group of phases. The transformations to CsCl-like phases are near 2 kbar in this case, following the empirical rule (*20*) that increasing cationic radius simulates higher pressures. Similarly, $CsNO_2$ does not occur in NaCl-like phases, but is found to be CsCl-like in all its presently known forms. A slight anomaly is the absence of a phase similar to KNO_2 VI in the phase diagrams of $CsNO_2$ and $RbNO_2$. This tetragonal high-pressure phase appears to be somewhat similar to KN_3, with an anionic disorder intermediate between those of KNO_2 IV and KNO_2 V (*18*). Since RbN_3 II and CsN_3 II are isostructural with KN_3 (*31*), there appears to be no obvious reason why a similar phase should not also be found for $RbNO_2$ and $CsNO_2$. This is, nevertheless, not the case.

A further matter of interest concerns the similarities between the phase diagrams of the alkali halides, cyanides, nitrites, azides and hydrofluorides. At high temperatures the less symmetrical anions usually have sufficient disorder to crystallize in the same space groups as the corresponding alkali halides, while at lower temperatures partial or complete ordering, more or less characteristic of the anion concerned, develops. However, even here many similarities can be found. Metastable rhombohedral NaCN (*32*) and possibly metastable KCN II (*11*, *33*) are closely related to rhombohedral KNO_2 II (*14*). $NaNO_2$ I, II, III and IV (*2–7*, *12*), NaCN II and III (*34*), KCN V (*35*) and $AgNO_2$ (*36*) all appear to be orthorhombic, space group D_{2h}^{25}–*Immm* or C_{2v}^{20}–*Im2m*, and to have closely related structures. There even appear to be similarities between monoclinic low-temperature RbCN, the metastable monoclinic phase of KCN (*25*), $RbNO_2$ II, KNO_2 III and VII (*16*). Similarly, in the group of denser phases KCN IV (*37*), CsCN II (*38*), KNO_2 IV (*18*), $CsNO_2$ II and probably $RbNO_2$ II are all rhombohedral with the same space group and closely related structures. KNO_2 VI appears to be closely related to KN_3 and KHF_2 II, as mentioned above.

Work is in progress to obtain X-ray diffraction patterns of the new high-pressure phases $RbNO_2$ III and IV.

Acknowledgments

The authors would like to thank Mrs. Martha C. Pistorius for writing the computer programs used in fitting the transition data and in indexing the X-ray powder patterns. Thanks are due to Dr. J. C. A. Boeyens, Dr. J. Coetzer and Dr. J. P. R. de Villiers of this Institute for valuable discussions. J. Erasmus and his staff and A. de Kleijn and his staff kept the apparatus in good repair, and were responsible for the manufacture of the furnace parts. Calculations were carried out on the IBM 360/65H of the National Research Institute for Mathematical Sciences.

References

1. S. Sawada, S. Nomura, S. Fujii, and I. Yoshida, *Phys. Rev. Lett.* **1**, 320 (1958).
2. M. R. Truter, *Acta Crystallogr.* **7**, 73 (1954).
3. C. B. Carpenter, *Acta Crystallogr.* **5**, 132 (1952); **8**, 852 (1955).
4. M. I. Kay and B. C. Frazer, *Acta Crystallogr.* **14**, 56 (1961).
5. S. Hoshino, *J. Phys. Soc. Jap.* **19**, 140 (1964).
6. Y. Yamada, I. Shibuya, and S. Hoshino, *J. Phys. Soc. Jap.* **18**, 1594 (1963).
7. M. I. Kay, B. C. Frazer, and R. Ueda, *Acta Crystallogr.* **15**, 506 (1962).
8. K. Gesi, K. Osawa, and Y. Takagi, *J. Phys. Soc. Jap.* **20**, 1773 (1965).
9. E. Rapoport, *J. Chem. Phys.* **45**, 2721 (1966).
10. C. W. F. T. Pistorius, E. Rapoport, and J. B. Clark, *Z. Phys. Chem. (Frankfurt)* **59**, 200 (1968).
11. P. W. Bridgman, *Proc. Amer. Acad. Arts Sci.* **72**, 45 (1937).
12. K. Gesi, *J. Phys. Soc. Jap.* **26**, 953 (1969).
13. J. D. Ray, *J. Inorg. Nucl. Chem.* **15**, 290 (1960).
14. J. K. Solbakk and K. O. Strømme, *Acta Chim. Scand.* **23**, 300 (1969).

15. S. TANISAKI AND T. ISHIMATSU, *J. Phys. Soc. Jap.* **20**, 1277 (1965).
16. C. W. F. T. PISTORIUS AND P. W. RICHTER, *Z. Anorg. Allg. Chem.*, in press.
17. J. D. RAY AND R. A. OGG, *J. Phys. Chem.* **60**, 1599 (1965).
18. C. W. F. T. PISTORIUS, *High Temp. High Pressures*, in press.
19. A. FERRARI, L. CAVALCA, AND M. E. TANI, *Gazz. Chim. Ital.* **87**, 310 (1957).
20. C. W. F. T. PISTORIUS, *in* "Solids under Pressure," (H. Ll. D. Pugh, ed.), p. 97, Institution of Mechanical Engineers, London (1971).
21. G. C. KENNEDY AND P. N. LAMORI, *in* "Progress in Very High Pressure Research" (F. P. Bundy, W. R. Hibbard and H. M. Strong, eds.), p. 304, Wiley, New York (1961).
22. C. W. F. T. PISTORIUS AND J. B. CLARK, *High Temp. High Pressures* **1**, 561 (1969).
23. P. W. RICHTER AND C. W. F. T. PISTORIUS, *J. Solid State Chem.* **3**, 197 (1971).
24. R. D. SHANNON AND C. T. PREWITT, *Acta Crystallogr.* **B26**, 1046 (1970).
25. G. S. PARRY, *Acta Crystallogr.* **15**, 601 (1962).
26. D. M. NEWNS AND L. A. K. STAVELEY, *Chem. Rev.* **66**, 267 (1966).
27. W. A. BASSETT, T. TAKAHASHI, H. K. MAO, AND J. S. WEAVER, *J. Appl. Phys.* **39**, 319 (1968).
28. O. L. ANDERSON, *J. Phys. Chem. Solids* **27**, 547 (1966).
29. E. RAPOPORT, *J. Chem. Phys.* **46**, 2891 (1967).
30. J. B. CLARK AND E. RAPOPORT, *J. Chem. Phys.* **49**, 2453 (1968).
31. C. W. F. T. PISTORIUS, *J. Chem. Phys.* **51**, 2604 (1969).
32. L. A. SIEGEL, *J. Chem. Phys.* **17**, 1146 (1949).
33. C. W. F. T. PISTORIUS, J. B. CLARK, AND E. RAPOPORT, *J. Chem. Phys.* **48**, 5123 (1968).
34. C. W. F. T. PISTORIUS AND J. C. A. BOEYENS, *J. Chem. Phys.* **48**, 1018 (1968).
35. J. M. BIJVOET AND J. A. LELY, *Rec. Trav. Chim. Pays-bas* **59**, 908 (1940).
36. R. E. LONG AND R. E. MARSH, *Acta Crystallogr.* **15**, 448 (1962).
37. C. W. F. T. PISTORIUS, *J. Phys. Chem. Solids*, **32**, 2761 (1971).
38. J. A. LELY, Dissertation, Utrecht, Netherlands (1942).